

# Different Membrane Anchoring Positions of Tryptophan and Lysine in Synthetic Transmembrane $\alpha$ -Helical Peptides\*

(Received for publication, April 5, 1999, and in revised form, May 10, 1999)

Maurits R. R. de Planque<sup>‡§</sup>, John A. W. Kruijtz<sup>¶</sup>, Rob M. J. Liskamp<sup>¶</sup>, Derek Marsh<sup>||</sup>,  
Denise V. Greathouse<sup>\*\*</sup>, Roger E. Koeppe II<sup>\*\*</sup>, Ben de Kruijff<sup>‡</sup>, and J. Antoinette Killian<sup>‡</sup>

From the <sup>‡</sup>Department Biochemistry of Membranes, Center for Biomembranes and Lipid Enzymology, Institute of Biomembranes, Utrecht University, Padualaan 8, 3584 CH Utrecht, The Netherlands, the <sup>¶</sup>Department of Medicinal Chemistry, Utrecht University, Sorbonnelaan 16, 3584 CA Utrecht, The Netherlands, <sup>||</sup>Abteilung Spektroskopie, Max-Planck-Institut für biophysikalische Chemie, D-37077 Göttingen, Germany, and the <sup>\*\*</sup>Department of Chemistry and Biochemistry, University of Arkansas, Fayetteville, Arkansas 72701

**Specific interactions of membrane proteins with the membrane interfacial region potentially define protein position with respect to the lipid environment. We investigated the proposed roles of tryptophan and lysine side chains as “anchoring” residues of transmembrane proteins. Model systems were employed, consisting of phosphatidylcholine lipids and hydrophobic  $\alpha$ -helical peptides, flanked either by tryptophans or lysines. Peptides were incorporated in bilayers of different thickness, and effects on lipid structure were analyzed. Induction of nonbilayer phases and also increases in bilayer thickness were observed that could be explained by a tendency of Trp as well as Lys residues to maintain interactions with the interfacial region. However, effects of the two peptides were remarkably different, indicating affinities of Trp and Lys for different sites at the interface. Our data support a model in which the Trp side chain has a specific affinity for a well defined site near the lipid carbonyl region, while the lysine side chain prefers to be located closer to the aqueous phase, near the lipid phosphate group. The information obtained in this study may further our understanding of the architecture of transmembrane proteins and may prove useful for refining prediction methods for transmembrane segments.**

In biological membranes, a variety of interactions can occur between lipids and proteins that affect protein as well as lipid properties and in which both the hydrophobic membrane core and the more polar membrane interfaces can be involved (1–3). Membrane proteins are able to span the lipid bilayer through interactions of their exposed hydrophobic segments with the lipid hydrocarbon acyl chains. In general, the length of these hydrophobic segments will approximately match the membrane hydrophobic thickness. However, also a mismatch between protein hydrophobic length and membrane hydrophobic thickness may occur. Such a mismatch can have considerable influence on membrane structure and function (reviewed in Ref. 4) and may, for example, be involved in protein sorting,

microdomain formation, changes in protein activity, or changes in lipid structure and organization.

In contrast to the hydrophobic core of a membrane, the membrane interface presents a complex and heterogeneous chemical environment, which accounts for a relatively large proportion of the total bilayer thickness (3). Specific interactions of membrane proteins with the interfacial region of the lipids may influence many functional processes, such as for instance membrane protein assembly, topology of membrane proteins, the mode of protein insertion into the membrane, and protein anchoring to the membrane. In addition, such interactions may play a determining role in hydrophobic mismatch (4).

Analyses of the structure of transmembrane proteins suggest that two types of amino acids may be of special importance for interactions of membrane proteins with the interfacial region: aromatic amino acids, in particular tryptophans, which are enriched at both ends of transmembrane fragments (5–9) and appear to have a preferred interaction with the interface (10), and charged residues, which also are preferentially located near the membrane interfaces (11). Positively charged residues interact with negatively charged phospholipids and are predominantly positioned at the cytoplasmic side, according to the positive inside rule (11).

In this study, we aim to investigate the role of interfacially localized aromatic tryptophans and positively charged lysines in protein-membrane interfacial interactions by using a strategy that is based on hydrophobic mismatch effects. We shall employ artificial peptides of variable hydrophobic length, flanked by either tryptophan or lysine residues. These peptides will be incorporated in lipid bilayers of varying thickness, allowing a wide range of mismatch situations. Upon creating such a hydrophobic mismatch, it can be expected that the lipid structure will readjust if the residues flanking the hydrophobic segment of the peptide prefer to maintain interactions with the lipid head group region. Analysis of the effects on lipid organization will thus provide information on the interaction of these flanking residues with the interfacial region.

Indeed, we have shown earlier, using simple model systems, that hydrophobic mismatch can result in complementary lipid conformational changes (10, 12). It was concluded that the affinity of flanking tryptophan residues for the interface might be important in determining both the nature and extent of changes in lipid organization. In the present study, we compared the effect of tryptophan and lysine as flanking residues on lipid structure. Striking differences were observed between the membrane-associating and lipid-modulating properties of Lys- and Trp-flanked model peptides. The results suggest that tryptophan residues prefer to be located in a well defined region at the polar/apolar interface in phosphatidylcholine bi-

\* This work was supported by the Council for Chemical Sciences with financial aid from the Netherlands Organization for Scientific Research, by National Institutes of Health Grant GM 34968 (to R. E. K. and D. V. G.), by NATO Grant CRG 950357, and by EMBO Fellowship ASTF 8778 (to M. R. R. de P.). The costs of publication of this article were defrayed in part by the payment of page charges. This article must therefore be hereby marked “advertisement” in accordance with 18 U.S.C. Section 1734 solely to indicate this fact.

§ To whom correspondence should be addressed. Tel.: 31-30-2535512; Fax: 31-30-2522478; E-mail: m.r.r.deplanque@chem.uu.nl.

TABLE I  
Amino acid sequences of the peptides used

Peptide	Sequence
KALP16	Acetyl-GKKLALALALAKKA-amide
KALP19	Acetyl-GKKLALALALALAKKA-amide
KALP23	Acetyl-GKKLALALALALALALAKKA-amide
WALP16	Acetyl-GWWLALALALAWWA-ethanolamine
WALP19	Acetyl-GWWLALALALALALAWWA-ethanolamine
WALP23	Acetyl-GWWLALALALALALALAWWA-ethanolamine

layers near the lipid carbonyls, while lysine residues prefer to be localized near the more polar region around the lipid phosphate group or more outward toward the aqueous phase.

#### EXPERIMENTAL PROCEDURES

##### Materials

WALP<sup>1</sup> peptides (see Table I) were synthesized by previous methods (10, 13), except that acetyl-Gly was used in place of formyl-Ala as the N-terminal residue, and the resin cleavage step was performed using ethanolamine at room temperature (14). When necessary (<90% purity), peptides were purified by HPLC. The identity of the peptides was confirmed by fast atom bombardment mass spectrometry or electrospray mass spectrometry.

The KALP peptides (Table I) were synthesized on an automatic ABI 433A peptide synthesizer using the ABI FastMoc 0.25 mmol protocols (49, 50), except that the coupling time was 45 min instead of 20 min. Fmoc (*N*-(9-fluorenyl)methoxycarbonyl) amino acid derivatives, activated *in situ* using 2-(1H-benzotriazole-1-yl)-1,1,3,3-tetramethyluronium hexafluorophosphate/1-hydroxybenzotriazole and *N,N'*-diisopropylethylamine in *N*-methylpyrrolidinone, were used in the coupling steps. The peptide was deprotected and cleaved from the resin by treatment with 10 ml of trifluoroacetic acid, 0.25 ml of H<sub>2</sub>O, and 0.25 ml of triisopropylsilane for 2 h at room temperature. Finally, the peptide was precipitated in a methyl *tert*-butyl ether/*n*-hexane (1:1, v/v) solution. After this, the pellet was dissolved in *tert*-butanol/water (1:1, v/v) (~60 ml) and lyophilized to obtain the crude peptide as a white fluffy solid, which was ≥90% pure according to analytical HPLC. The identity of the peptides was confirmed by fast atom bombardment mass spectrometry or electrospray mass spectrometry.

All of the phospholipids were purchased from Avanti Polar Lipids Inc. (Birmingham, AL). Deuterium-depleted water was from Isotec Inc. (Miamisburg, OH). *n*-(*N*-Oxy-4,4-dimethylloxazolidin-2-yl) stearic acid (*n*-SASL) isomers were synthesized according to Hubbell and McConnell (15).

##### Methods

**Sample Preparation**—The procedure followed for WALP analogs is identical to methods used in earlier work (10, 12). WALP analogs, quantified by the absorbance of tryptophan at 280 nm, were predissolved in 10 μl of trifluoroacetic acid/mg of peptide and were two times dissolved in 1 ml of trifluoroethanol, followed by drying in a rotary evaporator. Unless stated otherwise, the peptides were dissolved in 0.5 ml of trifluoroethanol and added, at temperatures above the gel to liquid crystalline phase transition, to 0.5 ml of a lipid suspension in distilled water, followed by the addition of 10 ml of water and immediate lyophilization. For some experiments, a mixed film method was used, in which the similarly treated peptide was added to 0.5 ml of a lipid suspension in methanol, followed by drying in a rotary evaporator and overnight incubation under high vacuum. Control experiments showed that both methods yielded identical results (data not shown). KALP peptides were quantified by their dry weight, and samples were prepared with the mixed film method. Further sample preparation depended on the kind of measurement (see below).

<sup>1</sup> The abbreviations used are: WALP, tryptophan-alanine-leucine peptide Ac-GW<sub>2</sub>(LA)<sub>n</sub>W<sub>2</sub>A-ethanolamine; ESR, electron spin resonance; KALP, lysine-alanine-leucine peptide Ac-GK<sub>2</sub>(LA)<sub>n</sub>K<sub>2</sub>A-amide; PC, phosphatidylcholine; 18:1<sub>c</sub>-PC, 1,2-dioleoyl-*sn*-glycero-3-phosphocholine; 20:1<sub>c</sub>-PC, 1,2-dieicosenoyl-*sn*-glycero-3-phosphocholine; 22:1<sub>c</sub>-PC, 1,2-dierucoyl-*sn*-glycero-3-phosphocholine; 24:1<sub>c</sub>-PC, 1,2-dinervonoyl-*sn*-glycero-3-phosphocholine; 14:0-PC, 1,2-dimyristoyl-*sn*-glycero-3-phosphocholine; *n*-SASL, *n*-(*N*-oxy-4,4-dimethylloxazolidin-2-yl) stearic acid spin label; L<sub>v</sub>, liquid crystalline bilayer lipid phase; I, isotropic lipid phase, H<sub>II</sub>, inverse hexagonal lipid phase; HPLC, high pressure liquid chromatography.

**<sup>31</sup>P NMR Measurements**—Lipid/peptide mixtures with a 1:10 peptide/lipid molar ratio (containing 20 μmol of lipid) were hydrated in 1.5 ml of buffer (100 mM NaCl, 25 mM Tris, pH 7.4). Samples were spun down at 30,000 × *g* for 15 min at 4 °C, and the supernatant was removed. The pellet was washed with buffer if the pH of the supernatant was below pH 6. <sup>31</sup>P NMR spectra of the pellets were recorded on a Bruker MSL 300 spectrometer. The sample temperature was regulated using a Bruker B-VT1000 temperature controller. Proton-decoupled experiments were carried out at 121.5 MHz, with a 17-μs 90° pulse, a 1.3-s interpulse time, and gated proton-noise decoupling. A sweep width of 25 kHz, 1024 data points, and a 100-Hz line broadening were used, and approximately 15,000 scans were acquired.

**Circular Dichroism**—CD samples of pure peptide were prepared by adding 1 ml of buffer (100 mM NaCl, 25 mM Tris, pH 7.4) to 1 μmol of peptide powder and subsequent vortexing. CD spectra were recorded without any further sample processing. Samples containing lipids were prepared as described above and were hydrated in 1 ml of buffer that was diluted with distilled water (1:1, v/v), unless otherwise stated, to obtain a better signal-to-noise ratio. These samples were then sonicated for 5 min with a 50% duty cycle and with an input power of 40 watts, using a Branson 250 tip sonicator. To pellet down titanium particles and any residual multilamellar lipid structures, the sonicated samples were next centrifuged at 30,000 × *g* for 15 min at 4 °C. Spectra of oriented peptide/lipid systems, hydrated with distilled water instead of buffer, were measured after spreading 40 μl of a sonicated sample on a quartz plate, followed by air drying. For all samples, CD measurements were carried out on a Jasco J-600 spectropolarimeter, using a 0.2-mm path length cell, 1-nm bandwidth, 0.2-nm resolution, 1-s response time, and a scan speed of 20 nm/min. Unless otherwise noted, spectra were recorded at room temperature.

**<sup>2</sup>H NMR Measurements**—Samples containing peptide and 10 μmol of *sn*-2 perdeuterated 14:0-PC at a 1:30 molar ratio were hydrated in 1 ml of deuterium-depleted water. The samples were spun down at 30,000 × *g* for 15 min at 4 °C, and the supernatant was removed. The pellet was washed with deuterium-depleted water if the pH of the supernatant was below pH 6. <sup>2</sup>H NMR spectra of the pellets were recorded on a Bruker MSL 300 spectrometer, using a high power probe with a 7.5-mm solenoidal sample coil. <sup>2</sup>H NMR measurements were performed at 46.1 MHz, using a quadrupolar echo sequence (16) with a 2.6-μs 90° pulse, a 50-μs pulse separation, a repetition rate of two acquisitions per second, and a spectral width of 417 kHz, with 2048 data points in the time domain. Approximately 80,000 scans were accumulated. The free induction decays were left-shifted to begin at the top of the echo, zero-filled to 8192 points, and multiplied with an exponential window function equivalent to a line broadening of 50 Hz. Spectra were recorded at 34 °C.

**Analysis of the <sup>2</sup>H NMR Spectra**—<sup>2</sup>H NMR powder spectra were dePaked as described earlier (12). This dePacking procedure results in spectra that would be obtained for an aligned membrane with its bilayer normal parallel to the magnetic field. It enhances the resolution and results in doublets with splittings Δ*ν*<sub>Q</sub> that relate to the segmental order parameter *S*(*i*). Order parameter profiles were obtained by assuming that the segmental order varies monotonically along the acyl chain. From these profiles, the effective length of the acyl chains was estimated as described (12).

**ESR Measurements**—Both KALP and WALP-containing samples were prepared by a mixed film method, as described earlier (12). Dried peptide/14:0-PC films (containing 1.5 μmol of lipid) with a 1:30 or 1:10 molar ratio, doped with 1 mol % of *n*-SASL, were hydrated in 40 μl of distilled water. Samples were spun down at 5000 × *g* for 15 min at room temperature in 1-mm inner diameter capillaries, which were flame-sealed after removal of the supernatant. ESR spectra were recorded on a Varian Century Line Series 9-GHz spectrometer equipped with a nitrogen gas flow temperature regulation system. Sample-containing capillaries were accommodated within standard 4-mm quartz ESR tubes containing light silicone oil for thermal stability. Temperature was measured by a fine wire thermocouple located at the top of the microwave cavity within the silicone oil. Conventional, in-phase ESR spectra were recorded at 34 °C, at a modulation amplitude of 1.6 G peak-to-peak and a modulation frequency of 100 kHz with a sweep width of the static field of 100 G.

#### RESULTS

**Effects of Short KALP and WALP Analogs on Lipid Phase Behavior**—In a previous study, we showed that short tryptophan-flanked peptides have a pronounced effect on lipid conformation, inducing inverted hexagonal (H<sub>II</sub>) phases at high

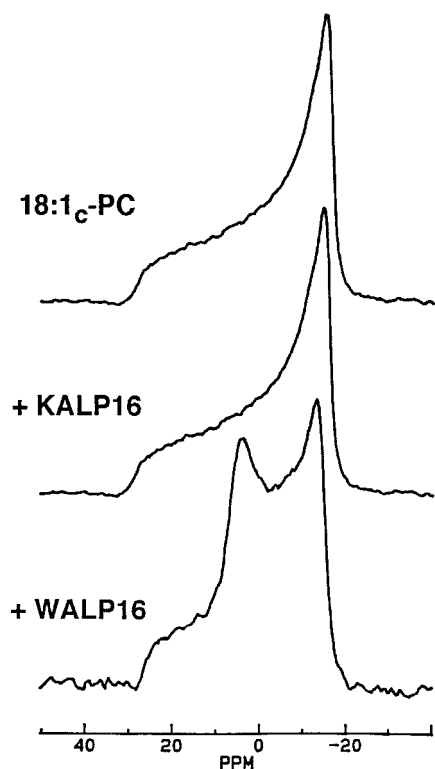


FIG. 1.  $^{31}\text{P}$  NMR spectra of dispersions of 18:1<sub>c</sub>-PC in the absence and presence of KALP16 or WALP16, as indicated in the figure, at a molar peptide/lipid ratio of 1:10 at 30 °C.

concentration in bilayer-preferring phosphatidylcholine lipids. To discover whether this behavior is a unique property of Trp-flanked peptides, we first compared the effect of the lysine-containing peptide KALP16 on the phase behavior of 18:1<sub>c</sub>-PC lipids with that of the tryptophan-containing peptide WALP16.  $^{31}\text{P}$  NMR spectra of these systems at a 1:10 peptide/lipid molar ratio are shown in Fig. 1. Pure 18:1<sub>c</sub>-PC gives a spectrum with a low field shoulder and a high field peak, typical for the preferred planar bilayer organization of this lipid in the liquid crystalline ( $L_{\alpha}$ ) phase (17, 18). WALP16 associates completely with the lipids and partially induces an  $H_{II}$  phase, as characterized by the spectral component with inverted asymmetry and a 2-fold reduced residual chemical shift anisotropy compared with the  $L_{\alpha}$  spectrum (17, 18). Although KALP16 has the same backbone length as WALP16, it does not change the lamellar phase preference of this lipid. This strikingly different behavior suggests that the Lys-flanked peptides either are unable to induce nonbilayer phases in PC or do not incorporate in the membrane.

**Solubility Properties and Conformational Behavior of KALP and WALP Analogs**—It is possible that KALP16, which is less hydrophobic than WALP16, does not incorporate into the membrane because it is soluble in buffer. To investigate the behavior of KALP and WALP analogs in buffer solution, circular dichroism measurements were performed. CD spectra of dried peptide films, hydrated with buffer, are shown in Fig. 2. A clear solution of WALP16 in buffer could not be achieved, and the CD signals obtained were equivalent to the background signal, indicating that all of the WALP had aggregated. A similar behavior was observed for WALP23 (data not shown). In contrast, both KALP16 and KALP19 formed clear solutions in buffer and gave well defined CD spectra corresponding to 15 and 40%  $\alpha$ -helix, respectively, indicating that the longer peptide forms a more stable helix, as is commonly observed (*e.g.* Ref. 19). KALP23 again did not give a clear solution, and only

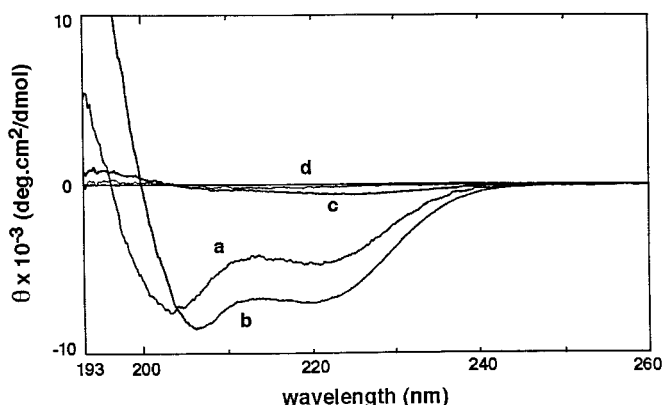


FIG. 2. Circular dichroism spectra of KALP16 (a), KALP19 (b), KALP23 (c), and WALP16 (d) in buffer at a concentration of 1 mM at room temperature.

a very weak signal was observed, suggesting that this longer peptide is too hydrophobic to solubilize in the buffer solution. These results suggest that short KALP peptides prefer not to associate with the membrane because they are soluble in buffer solution. Indeed, spinning down the KALP16/18:1<sub>c</sub>-PC NMR sample yielded a supernatant with a CD spectrum (not shown) that was very similar to that of pure KALP16 in Fig. 2. Thus, longer KALP peptides are required to establish whether Lys-flanked peptides are capable of inducing nonbilayer phases and/or changes in lipid chain configuration in phosphatidylcholine membranes.

**Effects of Longer KALP and WALP Analogs on Lipid Phase Behavior**—The KALP23 analog has little structure in buffer solution but adopts an  $\alpha$ -helical conformation in a lipid environment (see below), also in the presence of the longest lipids used in this study (data not shown). This indicates solubilization of (at least a large fraction of) KALP23 in a membrane environment under mismatch conditions (see also Refs. 20 and 21). To investigate the consequences of mismatch on lipid phase behavior, 20:1<sub>c</sub>-, 22:1<sub>c</sub>-, and 24:1<sub>c</sub>-PC were selected, which have a large bilayer thickness compared with the length of KALP23 and corresponding WALP analogs. The  $^{31}\text{P}$  NMR spectra of KALP23 and of WALP23, WALP21, and WALP19 at a 1:10 molar ratio of peptide to lipid are shown in Fig. 3. Spectra were recorded at both 30 and 60 °C to investigate the temperature dependence of the lipid phase modulation. In the absence of peptide, all lipids depicted are in the  $L_{\alpha}$  phase. The spectrum of KALP23 in 24:1<sub>c</sub>-PC at 30 °C has components in the line shape that deviate from that of a bilayer phase but cannot be interpreted unambiguously in terms of nonbilayer phases. It does confirm, however, that the peptide is associated with the membrane. Raising the temperature to 60 °C results in a line shape that contains a component clearly representative of a  $H_{II}$  phase. This has not previously been reported for Lys-based transmembrane peptides and indicates the ability of these peptides to induce  $H_{II}$  phase formation in PC in response to mismatch.

Also for KALP23 in the 20:1<sub>c</sub> and 22:1<sub>c</sub>-PC systems, a higher temperature is necessary to obtain resolution of the two spectral components, but in these systems an isotropic signal, most probably a cubic-like lipid phase (10), is obtained, together with an  $L_{\alpha}$  component. With even shorter lipids, spectra at both temperatures are representative of pure  $L_{\alpha}$  phases (data not shown). This behavior is similar to that previously observed for short WALP peptides, which upon increasing the lipid length first induced an  $L_{\alpha} \rightarrow I$  transition and then, at larger mismatch, an  $I \rightarrow H_{II}$  transition. Both transitions are very sensitive to the exact length difference of the particular WALP/PC

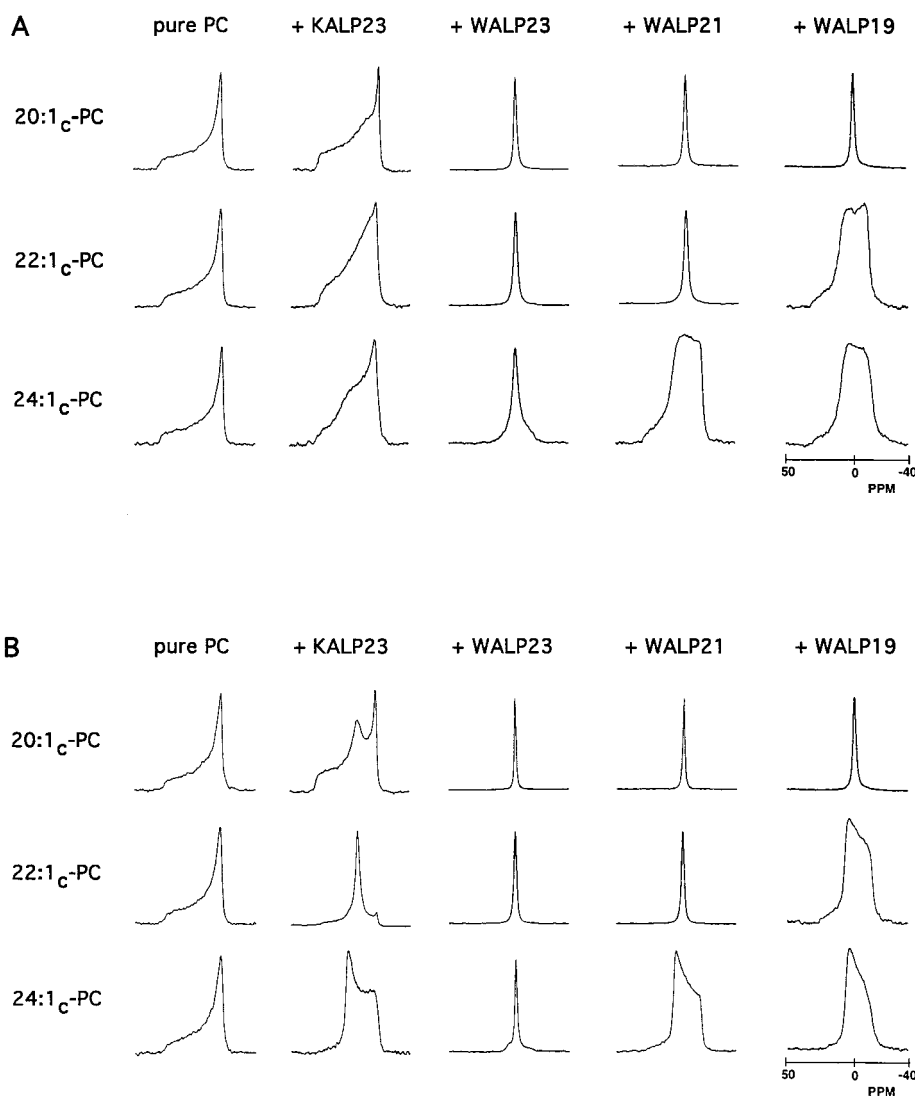


FIG. 3.  $^{31}\text{P}$  NMR spectra of dispersions of 20:1<sub>c</sub>, 22:1<sub>c</sub>, and 24:1<sub>c</sub>-PC, in the absence and presence of KALP23, WALP23, WALP21, or WALP19 at 30 °C (A) and 60 °C (B), as indicated in the figure, with a molar ratio of peptide to lipid of 1:10.

combination (10). Therefore, the effects on phase behavior can be used as a tool to compare the effective hydrophobic length of KALP23 with that of corresponding WALP analogs.

As shown in Fig. 3, the tryptophan peptide WALP23 behaves very differently from its corresponding Lys analog KALP23. WALP23 does not induce an H<sub>II</sub> phase and is much more efficient in inducing nonbilayer phases at lower temperature than is KALP23. Nearly or totally pure isotropic phases are formed already at room temperature in the three PC systems studied, and increasing the temperature has only a minor effect, in agreement with previous observations with shorter WALP analogs (22). The fact that an almost pure isotropic phase is induced in 24:1<sub>c</sub>-PC suggests a smaller mismatch with this membrane than in the case of KALP23 (see “Discussion”). To obtain more information about this mismatch difference, WALP peptides with a shorter hydrophobic length were also employed. With WALP21 and WALP19 (Fig. 3) the I → H<sub>II</sub> transition occurs between 22:1<sub>c</sub> and 24:1<sub>c</sub>-PC and between 20:1<sub>c</sub> and 22:1<sub>c</sub>-PC, respectively. From these data, it can be concluded that KALP23 has the same effect on the I → H<sub>II</sub> transition as a shorter WALP peptide, approximately equal to WALP21 and certainly longer than WALP19. Thus, KALP23 behaves as if it has the same hydrophobic length as a shorter WALP peptide, indicating that the effective hydrophobic length of the peptides is related to the nature of the flanking residues.

*Effects of Longer KALP and WALP Analogs on Bilayer Thick-*

*ness and Lipid Dynamics*—For studying mismatch-induced lipid deformation in situations where the peptide is relatively long with respect to the hydrophobic bilayer thickness, we investigated the ability of peptides to influence the molecular order of the lipid acyl chains, while the overall organization remains an L<sub>α</sub> lipid phase. To this end, KALP23 and WALP23 were incorporated at a 1:30 peptide/lipid molar ratio into bilayers of 14:0-PC with perdeuterated *sn*-2 chains.  $^{31}\text{P}$  NMR measurements confirmed that the lipids in these systems are in a bilayer organization, and the effects of the peptides on acyl chain order were characterized by  $^2\text{H}$  NMR.

Fig. 4 presents the  $^2\text{H}$  NMR spectra of 14:0-PC bilayer dispersions, with and without KALP23 or WALP23. Visual inspection of the spectrum representing the KALP23/14:0-PC system reveals a very small increase in quadrupolar splittings for the central methyl and the outer methylene peaks, relative to the pure 14:0-PC. These splittings are significantly larger for the WALP23 peptide, suggesting that the tryptophan-based peptides thicken the 14:0-PC membrane more than do their lysine-based counterparts. Segmental order parameters  $S(i)$  were derived, and from these the mean hydrophobic thicknesses of the different lipid/peptide systems were quantified, as described under “Methods.” The resulting values are presented in Table II, together with the data obtained previously for WALP16 and WALP19. For the pure 14:0-PC system, a value of 22.5 Å was obtained, which is in fairly good agreement (within 1 Å) with

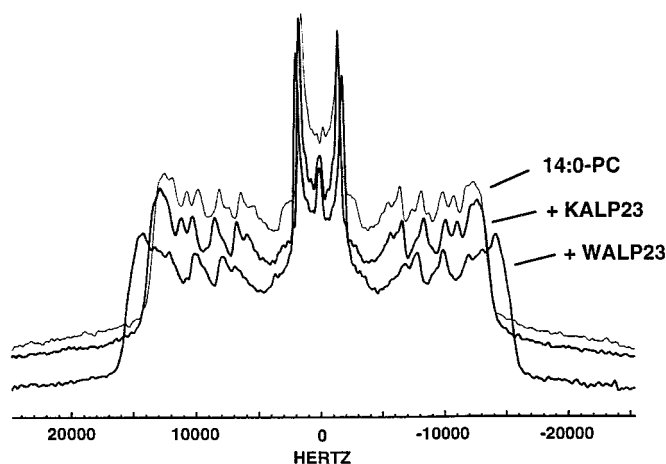


FIG. 4.  $^2\text{H}$  NMR spectra for peptide/14:0-PC- $d_{27}$  dispersions at a 1:30 molar ratio and at 34 °C. Spectra are shown without peptide (14:0-PC) and for samples containing the peptides indicated.

values based on x-ray measurements (23). Previously, we have shown for shorter WALP peptides that the 14:0-PC bilayer thickness increases with increasing peptide length, giving small but very systematic effects (12). The longer WALP23 analog continues this trend, but the effect of the lysine-based KALP23 peptide is even smaller than that of the shortest WALP analog. Thus WALP peptides are more effective modulators of 14:0-PC bilayer thickness than are KALP analogs. However, direct comparison of the effects of WALP23 and KALP23 is only possible when these peptides incorporate in 14:0-PC membranes with the same efficiency, have similar orientations with respect to the bilayer normal, and are in a similar aggregation state. We therefore analyzed these systems by CD and by ESR. The latter technique additionally yields information about the influence of the peptides on lipid dynamics.

CD spectra of both peptides at a 1:30 peptide/14:0-PC molar ratio at 34 °C are shown in Fig. 5. Both KALP23 and WALP23 are in an  $\alpha$ -helical conformation (curves *a*), as deduced from the minima near 222 and 208 nm, the crossover at 202 nm, and the maximum near 192 nm (24). From the spectral intensities, it can be concluded that equivalent amounts of KALP23 and WALP23 are associated with the membrane. The oriented spectrum (curve *b*) of KALP23 is characteristic of a helix with its long axis parallel to the incoming light (25). This implies a transmembrane orientation, perhaps with a minor tilt angle (<10 degrees) with respect to the bilayer normal, as judged from reference spectra that were calculated with the method described by De Jongh *et al.* (25). The oriented spectrum of WALP23 has an identical crossover point but a shifted minimum with respect to the spectrum corresponding to KALP23. The different line shape in the 220–235-nm region may be related to the tryptophan side chain chromophores in WALP23, which contribute to the CD signal in this spectral region (26). Thus, it can be concluded that both WALP23 and KALP23 are incorporated to equivalent extents as transmembrane  $\alpha$ -helical peptides in 14:0-PC without a significant tilt angle with respect to the bilayer normal.

ESR spectra of systems doped with spin-labeled lipid probes (*n*-SASL) were recorded to investigate the restriction of chain dynamics by KALP23 and WALP23 in 14:0-PC. Peptide assemblies that specifically restrict the rotational motion of the lipid acyl chains, induce a “restricted” ESR spectral component, which has been related to the peptide aggregational state (27, 28). Samples were first prepared with a 1:30 molar ratio of peptide to lipid. The resultant spectra were rather similar to

TABLE II

Changes in mean hydrophobic thickness ( $\Delta d$ ) relative to the pure *sn*-2 chain perdeuterated 14:0-PC, for systems at a 1:30 molar ratio of peptide to lipid and in anisotropy of the hyperfine splittings,  $\Delta(A_{\max} - A_{\min})$ , of the 14-SASL spin label relative to 14:0-PC systems at a 1:10 peptide/lipid molar ratio.

Measurements were performed at 34 °C, 10 °C above the main phase transition temperature of the pure 14:0-PC. The estimated experimental precision in hydrophobic thickness is  $\pm 0.1$  Å, and the precision in  $\Delta(A_{\max} - A_{\min})$  is  $\pm 0.2$  G.

Peptide	$\Delta d$	$\Delta(A_{\max} - A_{\min})$
	Å	G
WALP16	+0.4 <sup>a</sup>	+1.3 <sup>a</sup>
WALP19	+0.6 <sup>a</sup>	+2.5 <sup>a</sup>
WALP23	+1.0	+3.4
KALP23	+0.2	+1.8

<sup>a</sup> Value obtained from De Planque *et al.* (12).

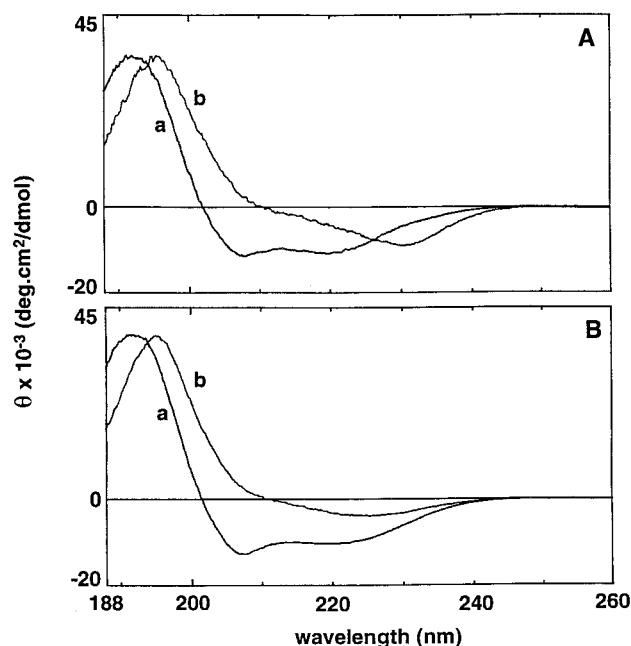


FIG. 5. Circular dichroism spectra of WALP23 (A) and KALP23 (B) in 14:0-PC at a 1:30 molar ratio of peptide to lipid at 34 °C in sonicated vesicles in excess water (*a*) and oriented bilayers (*b*). The ellipticity of the oriented spectra (*b*) is not absolute and is scaled to that of the nonoriented spectra (*a*).

those of the pure lipid (data not shown), and apparently overall lipid dynamics were not severely affected at this ratio, as deduced from the spectral line widths in the absence of peptide. The peptide concentration was therefore increased to 10 mol %, yielding the spectra depicted in Fig. 6. Pure 14:0-PC with 14-SASL in the  $L_{\alpha}$  phase is characterized by a spectrum with three sharp, symmetrical, quasi-isotropic peaks. Substantial changes in both line shape and anisotropy of the hyperfine splitting were observed upon incorporation of WALP23 and to a lesser extent on incorporation of KALP23; *i.e.* WALP23 influences the lipid order and dynamics to a considerably higher degree than does KALP23 (note the higher degree of asymmetry in the high field peak). The ESR results on peptide-induced changes in lipid chain motion parallel the trends observed in the  $^2\text{H}$  NMR experiments. The increase in spectral anisotropy,  $\Delta(A_{\max} - A_{\min})$  of 14-SASL, in the presence of the various peptides, is compared with the  $^2\text{H}$  NMR results in Table II. A similar ordering in the values of  $\Delta(A_{\max} - A_{\min})$  is also found for the 5-SASL spin label, in which the ESR reporter group is positioned closer to the polar end of the chain (data not shown, but see Ref. 12). However, even at the relatively high peptide/

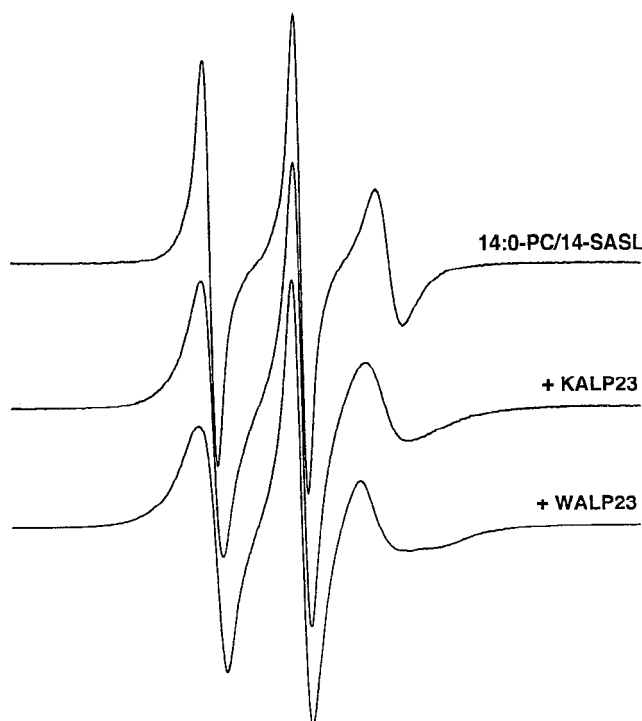


FIG. 6. ESR spectra of the 14-SASL stearic acid spin label in 14:0-PC, in the absence and in the presence of the peptides indicated, at a peptide/lipid molar ratio of 1:10 and 34 °C (total scan width = 100 G).

lipid molar ratio used, there is no evidence for a second, more motionally restricted spin-labeled lipid component,<sup>2</sup> such as is generally observed for spin labels at the 14-C atom position with large integral proteins or oligomeric transmembrane peptides (2, 29). Only when the peptide/lipid molar ratio in 14:0-PC was increased to 1:6, for which peptide aggregation might be expected, was there an indication of a motionally restricted population of 14-SASL at 30 °C. The inference that can be drawn from these results is that, at the molar ratio used in the <sup>2</sup>H NMR studies, both KALP23 and WALP23 are probably present as monomeric transmembrane helices and not as extensive oligomers.

#### DISCUSSION

In this study, we investigated the roles of tryptophan and lysine side chains as interfacial “anchoring” residues in transmembrane protein segments. Systems were created with a hydrophobic mismatch between peptides and lipids, and effects on lipids were studied. Striking differences in response were observed for both families of peptides. Here we will discuss these results and their implications.

**Effects on Lipid Structure of Relatively Short Peptides**—The situation of having progressively shorter WALP or KALP peptides incorporated into PC model membranes is equivalent to the situation in which either Trp or Lys is gradually moved toward the hydrophobic membrane region. The observed formation of nonbilayer phases as a response to such a hydrophobic mismatch can be understood on the basis that such nonbilayer structures contain areas of reduced hydrophobic “membrane” thickness, that better match the hydrophobic length of relatively short peptides (10).

It was found that both KALP23 and WALP23 are capable of

<sup>2</sup> ESR experiments were also performed with 18:1<sub>c</sub>-PC as host lipid. Again neither WALP23 nor KALP23, at a 1:10 peptide/lipid molar ratio, induced a motionally restricted component in spectra of the 14-SASL spin probe in these lipids at 30 °C.

TABLE III

Distance from the bilayer center of characteristic groups of 24:1<sub>c</sub>-PC and 14:0-PC in the liquid crystalline state and of the position of characteristic side chain groups of KALP23, WALP23, and WALP21 analogs

Average lipid phosphate positions were obtained by x-ray diffraction (23) and were extrapolated to C=O positions based on combined x-ray and neutron diffraction data of 18:1<sub>c</sub>-PC (35, 36). Amino acid side chain positions were taken from peptide models built using InsightII (version 98.0, Molecular Simulations Inc., San Diego, CA), based on an ideal  $\alpha$ -helical conformation. The resulting WALP23 model was energy-minimized using Discover (Molecular Simulations). The average position of the two terminally located Trp or Lys residues (see “Discussion”) is given.

Lipids	C=O	PO <sub>4</sub> <sup>-</sup>
14:0-PC	13	17
24:1 <sub>c</sub> -PC	20	24
Peptides	Trp NH	Lys $\epsilon$ -NH <sub>3</sub> <sup>+</sup>
WALP21	15.6	19.0
WALP23	17.1	
KALP23		

inducing nonbilayer phases, demonstrating that this lipid-modulating effect is not specific for Trp-flanked peptides. Furthermore, KALP23 induces essentially the same nonbilayer phases as the shorter WALP21. This shows that the effective hydrophobic length of the peptides is dependent on the nature of the flanking residues. This is supported also by studies on a WALP analog with the same total length but with its tryptophan residues shifted one position inward.<sup>3</sup> These studies indicated that the effects on PC organization depend on the distance between the Trp residues and not on the total peptide length, suggesting that indeed the flanking Trp residues delimit the peptide hydrophobic stretch.

The results obtained in the present study allow us to interpret the lipid-modulating properties of relatively short KALP and WALP peptides in terms of Lys and Trp location in the membrane. Such an interpretation requires consideration of the orientations of these side chains in a lipid environment. Space-filling models of WALP23 and KALP23 were built. The Trp torsion angles were based on the structure of membrane-embedded gramicidin (30, 31), in which the imino moiety of the rigid Trp indole side chain is pointing outward to the aqueous phase, an orientation that is also proposed for membrane-associating indole analogs (32). The flanking Lys side chains in KALP23 are modeled with the charged terminus pointing toward the aqueous phase. This Lys “snorkling” has been proposed for relatively short peptides, to avoid the burying of charges in the hydrophobic membrane core (33, 34). Resulting peptide dimensions are given in Table III.

When comparing the two peptides, the Lys  $\epsilon$ -NH<sub>3</sub><sup>+</sup> group extends about 1.9 Å farther from the membrane center than does the Trp indole NH. KALP23 induces nonbilayer phases similar to those of WALP21. This implies an additional difference of one residue at each end of the peptide, corresponding to a side chain extension of 1.5 Å (in an  $\alpha$ -helical conformation). Thus, adding the two factors, we conclude that the localization that is still favorable for a Lys  $\epsilon$ -NH<sub>3</sub><sup>+</sup> in a lipid bilayer is approximately 3.4 Å closer to the aqueous phase than that of a Trp NH. In a fluid phase PC bilayer, this distance corresponds approximately to the spacing between the lipid carbonyl and phosphate groups (Table III).

In 24:1<sub>c</sub>-PC, WALP21 and KALP23 induce an H<sub>II</sub> phase,

<sup>3</sup> M. R. R. de Planque, D. V. Greathouse, R. E. Koeppe II, and J. A. Killian, unpublished observations.

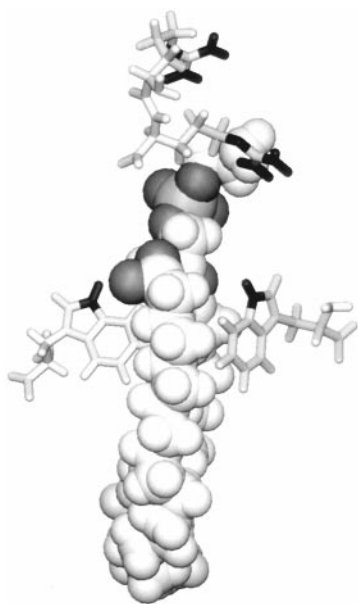


FIG. 7. Corey-Pauling-Koltun model of a phosphatidylethanolamine molecule embedded in the cytochrome  $bc_1$  complex (1BCC in the Protein Data Bank, Brookhaven National Laboratory, Upton, NY) from chicken heart inner mitochondrial membrane (48), with stick models of Trp<sup>C31</sup>, Trp<sup>C327</sup>, Arg<sup>G39</sup>, and Arg<sup>G40</sup>, which are in proximity to the lipid. The oxygen atoms (and phosphorus) of the lipid are shown in dark, as are the NH groups of the Trp and Arg side chains. Note that the tryptophans are located close to the glycerol oxygens, whereas the arginines are pointing toward the more polar regions of the lipid, above the phosphate group. The picture was generated using InsightII (Molecular Simulations).

indicating a large extent of hydrophobic mismatch. The expected positions of the Trp and Lys side chains for these peptides are well below the carbonyl and phosphate region in the 24:1<sub>c</sub>-PC bilayer, respectively (Table III). We propose that the Trp indole group disfavors a position with the imino moiety below the lipid carbonyl region and that the Lys  $\epsilon$ -NH<sub>3</sub><sup>+</sup> groups disfavor a position below the lipid phosphate region. Therefore, the positions of these side chains with respect to the membrane lipids would determine the extent of hydrophobic mismatch.

**Effects on Lipid Structure of Relatively Long Peptides**—With peptide/lipid combinations that are equivalent to moving the Lys and Trp residues outward in the direction of the aqueous phase, a different response of the membrane system is expected. WALP23 increases the bilayer thickness in this situation. As seen from the dimensions given in Table III, the tryptophans in this peptide would be located close to the polar lipid phosphate region in an unperturbed 14:0-PC bilayer. Because the lipid system responds to WALP23 incorporation with a stretch of its acyl chains, it is concluded that such a position of the Trp side chain is unfavorable and that Trp prefers a more hydrophobic interfacial environment. This is in accordance with water/membrane partitioning studies with small unstructured peptides (37).

KALP23 has only a small effect on acyl chain order and dynamics, in agreement with work on a comparable Lys-flanked polyleucine peptide (38, 39). Nevertheless, earlier studies have shown that Lys-flanked polyleucine peptides are capable of inducing systematic acyl chain ordering and disordering (40, 41). We conclude that little acyl chain stretch is observed in our system because the Lys side chains in KALP23 are in a favorable environment in 14:0-PC. The  $\epsilon$ -NH<sub>3</sub><sup>+</sup> groups of KALP23, in the extended snorkling conformation, are near the phosphates but slightly outwards toward the aqueous phase (Table III). However, the lysine side chains are flexible and, if not snorkling, they can stay even closer to the position

of the 14:0-PC phosphate region.

**Biological Significance: Preferred Interface Positions of Trp and Lys**—The selected combinations of peptides and lipids yield information about the positions of Trp and Lys side chains in transmembrane peptides. We propose that the tryptophan side chain has a specific affinity for a well defined site near the interface, with the indole imino moiety positioned near the center of the lipid carbonyl region, and the fused aromatic rings in contact with the lipid acyl chains. This location is in good agreement with the membrane depth of NH-containing carazole indole analogs, as determined by parallax analysis of fluorescence quenching (32, 42) but is on average somewhat deeper in the membrane than NMR studies on other small Trp analogs predict (43). In both studies, however, these water-soluble analogs are not part of a transmembrane peptide. It cannot be concluded whether the lysine  $\epsilon$ -NH<sub>3</sub><sup>+</sup> group has a specific affinity for the phosphate group. It is also possible that the side chain just prefers a sufficiently polar environment, which is offered by a broad interfacial region. Such an arrangement has been proposed for amphipathic model peptides (33, 34). We propose a model in which the Trp indole NH prefers a well defined position at the polar/apolar interface near the lipid carbonyl region, while the lysine  $\epsilon$ -NH<sub>3</sub><sup>+</sup> group is located in a more polar region, around the lipid phosphate group or slightly closer to the aqueous phase. Such a position would be stabilized by electrostatic  $\epsilon$ -NH<sub>3</sub><sup>+</sup>/phosphate interactions.

Analyses of protein x-ray structures have demonstrated that lipid-exposed transmembrane helices are enriched in aromatic and charged residues near the helix termini and that statistically the charged residues are positioned several Å closer to the termini than the aromatic residues (44). This is in agreement with our conclusions. Two x-ray structures of membrane proteins (cytochrome *c* oxidase (45, 46) and cytochrome  $bc_1$  complex (47, 48)) contain phospholipids, although these are embedded within the complex and are not adjacent to it. One of the two phosphatidylethanolamine lipids of the cytochrome  $bc_1$  complex is in proximity to two tryptophans and two arginines, as depicted in Fig. 7. The Trp indole moieties are in close contact with the lipid, with the indole NH groups adjacent to the lipid carbonyl moiety. The Arg side chains are positioned at a somewhat larger distance from the lipid and are oriented perpendicular to the acyl chains, with the terminal charge of Arg<sup>G40</sup> slightly above the phosphate group. These observations in a complex membrane protein are in full agreement with our conclusions from model studies on simple peptides.

Since this study provides for the first time information on the preferred positions of Trp and Lys relative to each other and relative to the interface, it might prove useful to incorporate our data explicitly in prediction methods for transmembrane segments of the many proteins for which the structure has not yet been solved.

**Acknowledgments**—We thank Gerda de Korte for HPLC analysis and Brigitta Angerstein for spin label synthesis.

#### REFERENCES

- Gil, T., Ipsen, J. H., Mouritsen, O. G., Sabra, M. C., Sperotto, M. M., and Zuckermann, M. J. (1998) *Biochim. Biophys. Acta* **1376**, 245–266
- Marsh, D., and Horváth, L. I. (1998) *Biochim. Biophys. Acta* **1376**, 267–296
- White, S. H., and Wimley, W. C. (1998) *Biochim. Biophys. Acta* **1376**, 339–352
- Killian, J. A. (1998) *Biochim. Biophys. Acta* **1376**, 401–416
- Landolt-Marticorena, C., Williams, K. A., Deber, C. M., and Reithmeier, R. A. F. (1993) *J. Mol. Biol.* **229**, 602–608
- Von Heijne, G. (1994) *Annu. Rev. Biophys. Biomol. Struct.* **23**, 167–192
- Reithmeier, R. A. F. (1995) *Curr. Opin. Struct. Biol.* **5**, 491–500
- Ostermeier, C., Iwata, S., and Michel, H. (1996) *Cur. Opin. Struct. Biol.* **6**, 460–466
- Doyle, D. A., Cabral, J. M., Pfuetzner, R. A., Kuo, A., Gulbis, J. M., Cohen, S. L., Chait, B. T., and MacKinnon, R. (1998) *Science* **280**, 69–77
- Killian, J. A., Salemink, I., De Planque, M. R. R., Lindblom, G., Koeppe, R. E., II, and Greathouse, D. V. (1996) *Biochemistry* **35**, 1037–1045
- Von Heijne, G. (1986) *EMBO J.* **5**, 3021–3027

12. De Planque, M. R. R., Greathouse, D. V., Koeppe, R. E., II, Schäfer, H., Marsh, D., and Killian, J. A. (1998) *Biochemistry* **37**, 9333–9345
13. Greathouse, D. V., Koeppe, R. E., II, Providence, L. L., Shobana, S., and Andersen, O. S. (1999) *Methods Enzymol.* **294**, 525–550
14. Goforth, R. L., Crawford, T., Van der Wel, P. C. A., Rhodes, N. E., Killian, J. A., and Greathouse, D. V. (1999) *Biophys. J.* **76**, A217
15. Hubbell, W. L., and McConnell, H. M. (1971) *J. Am. Chem. Soc.* **93**, 314–326
16. Davis, J. H., Jeffrey, K. R., Bloom, M., Valic, M. I., and Higgs, T. P. (1976) *Chem. Phys. Lett.* **42**, 390–394
17. Seelig, J. (1978) *Biochim. Biophys. Acta* **515**, 105–140
18. Cullis, P. R., and De Kruijff, B. (1979) *Biochim. Biophys. Acta* **559**, 399–420
19. Dieudonné, D., Gericke, G., Flach, C. R., Jiang, X., Farid, R. S., and Mendelsohn, R. (1998) *J. Am. Chem. Soc.* **120**, 792–799
20. Ren, J., Lew, S., Wang, Z., and London, E. (1997) *Biochemistry* **36**, 10213–10220
21. Webb, R. J., East, J. M., Sharma, R. P., and Lee, A. G. (1998) *Biochemistry* **37**, 673–679
22. Morein, S., Strandberg, E., Killian, J. A., Persson, S., Arvidson, G., Koeppe, R. E., II, and Lindblom, G. (1997) *Biophys. J.* **73**, 3078–3088
23. Lewis, B. A., and Engelman, D. M. (1983) *J. Mol. Biol.* **166**, 211–217
24. Greenfield, N., and Fasman, G. D. (1969) *Biochemistry* **8**, 4108–4116
25. De Jongh, H. H. J., Goormaghtigh, E., and Killian, J. A. (1994) *Biochemistry* **33**, 14521–14528
26. Chakrabarty, A., Kortemme, T., Padmanabhan, S., and Baldwin, R. L. (1993) *Biochemistry* **32**, 5560–5565
27. Marsh, D. (1993) in *New Compr. Biochem.* **25**, 41–66
28. Marsh, D. (1997) *Eur. Biophys. J.* **26**, 203–208
29. Marsh, D. (1985) in *Progress in Protein-Lipid Interactions* (Watts, A., and De Pont, J. J. H. H. M., eds) Vol. 1, pp. 143–172, Elsevier, Amsterdam
30. Hu, W., Lee, K. C., and Cross, T. A. (1993) *Biochemistry* **32**, 7035–7047
31. Koeppe, R. E., II, Killian, J. A., and Greathouse, D. V. (1994) *Biophys. J.* **66**, 14–24
32. Kachel, K., Asuncion-Punzalan, E., and London, E. (1995) *Biochemistry* **34**, 15475–15479
33. Mishra, V. K., Palgunachari, M. N., Segrest, J. P., and Anantharamaiah, G. M. (1994) *J. Biol. Chem.* **269**, 7185–7191
34. Mishra, V. K., and Palgunachari, M. N. (1996) *Biochemistry* **35**, 11210–11220
35. Wiener, M. C., and White, S. H. (1992) *Biophys. J.* **61**, 434–447
36. White, S. H. (1994) in *Membrane Protein Structure: Experimental Approaches* (White, S. H., ed) pp. 97–124, Oxford University Press, New York
37. Wimley, W. C., and White, S. H. (1996) *Nat. Struct. Biol.* **3**, 842–848
38. Roux, M., Neumann, J. M., Hodges, R. S., Devaux, P. F., and Bloom, M. (1989) *Biochemistry* **28**, 2313–2321
39. Subczynski, W. K., Lewis, R. N. A. H., McElhaney, R. N., Hodges, R. S., Hyde, J. S., and Kusumi, A. (1998) *Biochemistry* **37**, 3156–3164
40. Huschilt, J. C., Hodges, R. S., and Davis, J. H. (1985) *Biochemistry* **24**, 1377–1386
41. Nezil, F. A., and Bloom, M. (1992) *Biophys. J.* **61**, 1176–1183
42. Asuncion-Punzalan, E., Kachel, K., and London, E. (1998) *Biochemistry* **37**, 4603–4611
43. Yau, W.-M., Wimley, W. C., Gawrisch, K., and White, S. H. (1998) *Biochemistry* **37**, 14713–14718
44. Wallin, E., Tsukihara, T., Yoshikawa, S., Von Heijne, G., and Elofsson, A. (1997) *Prot. Sci.* **6**, 808–815
45. Tsukihara, T., Aoyama, H., Yamashita, E., Tomizaki, T., Yamaguchi, H., Shinzawa-Itoh, K., Nakashima, R., Yaono, R., and Yoshikawa, S. (1996) *Science* **272**, 1136–1144
46. Iwata, S., Ostermeier, C., Ludwig, B., and Michel, H. (1995) *Nature* **376**, 660–669
47. Iwata, S., Lee, J. W., Okada, K., Lee, J. K., Iwata, M., Rasmussen, B., Link, T. A., Ramaswamy, S., and Jap, B. K. (1998) *Science* **281**, 64–71
48. Zhang, Z., Huang, L., Shulmeister, V. M., Chi, Y. I., Kim, K. K., Hung, L. W., Crofts, A. R., Berry, E. A., and Kim, S. H. (1998) *Nature* **392**, 677–684
49. Applied Biosystems (1993) *Applied Biosystems Model 433A Peptide Synthesizer User's Manual*, Version 1.0, Applied Biosystems, Foster City, CA
50. Applied Biosystems (1993) *Applied Biosystems Research News*, pp. 1–12, Applied Biosystems, Foster City, CA



---

**MEMBRANES AND BIOENERGETICS:**  
**Different Membrane Anchoring Positions**  
**of Tryptophan and Lysine in Synthetic**  
**Transmembrane  $\alpha$ -Helical Peptides**

Maurits R. R. de Planque, John A. W.  
Kruijtzter, Rob M. J. Liskamp, Derek Marsh,  
Denise V. Greathouse, Roger E. Koeppe II,  
Ben de Kruijff and J. Antoinette Killian  
*J. Biol. Chem.* 1999, 274:20839-20846.  
doi: 10.1074/jbc.274.30.20839

---

Access the most updated version of this article at <http://www.jbc.org/content/274/30/20839>

Find articles, minireviews, Reflections and Classics on similar topics on the [JBC Affinity Sites](#).

Alerts:

- [When this article is cited](#)
- [When a correction for this article is posted](#)

[Click here](#) to choose from all of JBC's e-mail alerts

This article cites 47 references, 4 of which can be accessed free at  
<http://www.jbc.org/content/274/30/20839.full.html#ref-list-1>